International Journal of Academic Engineering Research (IJAER)
ISSN: 2643-9085
Vol. 10 Issue 8 August - 2026, Pages: 23-32

Development Prospects of Waste Thermal Energy Harvesting from Gas Flaring System using Thermoelectric Generators

Baribuma Gbaarabe

Department of Mechanical Engineering, Rivers State University, Port Harcourt, P.M.B 5080, Nigeria
buma3g@gmail.com

Abstract: *This study explores the development prospects of waste thermal energy harvesting from gas flaring systems using thermoelectric generators (TEGs). Thermal analysis indicates that radiative heat transfer is the primary mode of heat flux to the plate heat exchanger (PHE), consistent with elevated flare stack operating conditions. Although the radiative input of 970 kW is reduced to a net convective–conductive transfer rate of 489 kW due to cumulative thermal resistances, the system maintains a thermal effectiveness of 1.4%. Despite this relatively low effectiveness, the high flare thermal energy release of 106 MW translates into a recoverable waste heat potential of about 15 MW. The integrated thermoelectric harvesting (TEH) system is capable of generating 1.1MW of DC electrical power using 37,000 TEGs arranged in a series–parallel configuration, yielding 26MWh of usable energy per day, which can be stored in a 30MWh containerized energy storage system (CESS). Thermal simulations confirm effective heat propagation, with temperatures decreasing from 1200K at the flare tip to 600K across the PHE–TEG interface, ensuring uniform distribution and minimizing mismatch losses. Economic evaluation estimates a capital investment of $3.76 million with a simple payback period of 3 years, while environmental assessment projects an annual reduction of 5.44 million kg of* CO_2 *emissions. The findings demonstrate that TEH integration with flare systems is technically feasible, economically viable, and environmentally advantageous, offering a pathway for renewable power generation from flare waste heat while mitigating thermal pollution and carbon emissions.*

Keywords— Conductive-Convective-Radiative Heat Transfer, Flare Heat Released and Harvested, Gas Flaring System, Thermoelectric Generators (TEG), and Thermal Energy Harvesting (TEH).

1. INTRODUCTION (*Heading 1*)

Waste thermal energy is produced in various industrial processes, including fuel combustion and other exothermic chemical reactions. In combustion systems, fuels release a substantial quantity of thermal energy as a byproduct, which is often expelled into the environment despite its potential for reuse [1]. Gas flaring is the burning of natural gas and petroleum hydrocarbons in flare stacks by upstream oil industries in oil fields during operations. Gas flaring is a major source of greenhouse gas emissions and waste thermal energy, significantly contributing to global climate change and local thermal pollution [2]. The harvesting of the waste thermal energy from gas flaring systems offers a viable pathway to mitigate these environmental impacts by reducing the volume of heat discharged into the atmosphere and improving overall energy efficiency. Thermoelectric generators (TEGs) offer a means of harvesting and converting this waste thermal energy into usable electrical energy through the Seebeck effect. The Seebeck effect is the phenomenon where a temperature gradient across a thermoelectric material results in the generation of an electric energy. TEGs exploit this effect by utilizing a temperature gradient, with one side exposed to the waste heat source (hot side) and the other side cooled by ambient air or a cooling system (cold side). This temperature gradient drives the diffusion of charge carriers (electrons or holes) from the hot side to the cold side. This process establishes an electric potential difference, generating DC electrical power when a load is connected across the TEG terminals [3]. TEGs have evolved from their successful application in low-grade thermal energy harvesting for powering low-voltage systems such as wireless sensor networks, Internet of Things (IoT) devices, and deep-space probes, to more demanding domain of high-grade thermal energy harvesting. Although high-grade thermal sources offer significantly greater power generation potential, they introduce critical challenges, as TEGs must endure larger temperature gradients, elevated thermal stresses, and increased risks of material degradation under harsh operating conditions. However, recent advancements in thermoelectric materials and device design are effectively mitigating these limitations, enabling reliable operation at high temperatures. Notably, advanced materials such as skutterudites and half-Heusler alloys are increasingly replacing conventional bismuth telluride based materials for high-temperature applications, owing to their superior thermal stability and enhanced figures of merit (ZT) at temperatures exceeding 500°C [4]. The improvement in the performance of TEG had led to several researches on waste heat recovery from different sources using TEG, some of which are reviewed as follows:

Reference [5] reviews the potential of using TEG modules to recover waste heat from internal combustion engines. They propose a system comprising a plate-shaped heat exchanger, TEG modules, and a power converter, designed to be integrated with the engine's exhaust. The TEG modules capture waste heat from the exhaust gases, converting it into DC electrical energy. This energy is then transformed into AC by the power converter to operate an air conditioning system. The study concludes that the proposed waste heat recovery system not only enhances engine performance but also reduces emissions. Reference [6] reviews the principles and recent advancements in the development of thermoelectric materials for energy harvesting. Their analysis spans the evolution of thermoelectric materials, from foundational concepts to achieving high thermoelectric performance, as measured by the figure of merit. The authors emphasize that organic materials are leading the way in thermoelectric innovation, highlighting key advantages such as their lightweight properties, flexibility, cost-effectiveness, and scalability for large-scale energy production. They conclude that these attributes have the potential to significantly enhance the performance of TEG devices.

Reference [7] explores a new concept of power generation from TEGs using the exhaust airflow of HVAC system, along with solar radiation. They perform a parametric analysis of TEG thermal behavior under various conditions to generate significant temperature gradients and electrical power from TEGs in different practical configurations. Based on this analysis, they evaluate an innovative concept using an appropriate thermal model. The results show that this new power generation concept from TEGs is both economically viable and environmentally friendly. Reference [8] provide a review of waste heat recovery technologies, with a focus on advanced systems such as organic Rankine cycles, Kalina cycles, and combined cycles. They also examine emerging technologies, including thermoelectric, piezoelectric, thermionic, and thermophotovoltaic systems. The authors conclude that complex thermodynamic systems are highly effective for recovering waste heat and generating power on a large scale. Additionally, they highlight the potential of emerging technologies to directly convert waste heat into electricity for both small- and large-scale applications. Describing these innovations as the future of sustainable energy harvesting, the authors recommend further development of large-scale thermoelectric technology, which has yet to be fully commercialized. In the literatures reviewed, while TEGs are well established for waste heat recovery, their application to gas flaring systems remains largely unexplored. In view of the environmental and economic benefits associated with reducing gas flaring emissions [1], this study proposes a method for harvesting thermal energy from gas flaring systems and converting it into electrical energy through the integration of TEGs.

2. Materials and Methods

The materials used for this study include the design specifications of TEG module, data of thermophysical properties of flue gas and ambient air at the Soku gas plant base, design specifications of the existing flare stack, JANAF Thermochemical Tables and SOLIDWORKS simulation. The methods used in the study are described in the following subsections:

2.1 Description of the Case Study Gas Flaring System

The case study is based on the derrick-supported elevated flare stack at the Soku Gas Plant, operated by the Shell Petroleum Development Company (SPDC) Joint Venture in the coastal swamp region of the Niger Delta, Rivers State, Nigeria (4.7° N, 6.6° E). The facility is a key feed gas supplier to the Nigeria Liquefied Natural Gas (NLNG) terminal at Bonny Island, contributing up to 40 % of its feedstock with an installed processing capacity up to 1100 MMscf/d (≈245kg/s). Despite regulatory efforts to reduce routine flaring, gas flaring activity remained significant, with about 31 MMscf/d (≈7.2kg/s). At Soku and similar oil and gas facilities, flaring arises from variations in demand, infrastructure limitations, operational upsets, and intermittent disruptions to evacuation networks. The elevated flare serves to combust excess hydrocarbons safely, but this practice leads to substantial thermal energy release and greenhouse gas emissions that are of both environmental and economic consequence. The area is characterized by high ambient temperatures (annual average 26.55°C) and elevated humidity with minimal seasonal variation [9], [10]. Fig 2 illustrates the derrick-supported elevated flare system used for the safe combustion of excess hydrocarbon gases in oil and gas processing facilities. The system consists of a vertical flare stack centrally positioned within a steel lattice derrick structure that provides mechanical stability against wind and thermal loads. Waste gases are conveyed through the stack to the flare tip, where ignition occurs and combustion is sustained at an elevated height to enhance atmospheric dispersion and reduce ground-level thermal radiation. The flare stack has a cylindrical structure with effective diameter of 0.677m, total height of 35 m, and a structural weight of 16300kg. The flare stack and derrick structure are fabricated from carbon steel pipes. Structural connections are achieved using flange plates, connecting plates, and high-strength bolted joints between columns, beams, and braces. The typical composition of natural gas from the Soku gas field supplied to the processing plant is presented in Table 1.

Table 1: Composition of Natural Gas from Soku [11]

Composition	Volume (%)
CH_4	94.1532
C_2H_6	2.7801
C_3H_8	1.6582
C_4H_{10}	0.7791
C_5H_{12}	0.2971
N_2	0.1141
CO_2	0.2182

International Journal of Academic Engineering Research (IJAER)
ISSN: 2643-9085
Vol. 10 Issue 8 August - 2026, Pages: 23-32

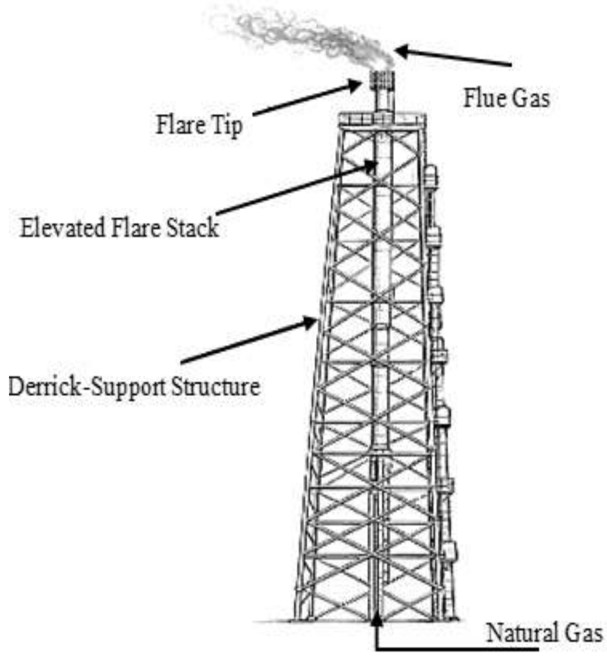

Fig.2: *Derrick-supported elevated flare stack [12]*

2.2 Description of the Case Study Gas Flaring System

An existing gas flaring system is redesigned to incorporate the TEH system as shown in Fig 3. The redesigned gas flaring system enables the conversion of waste heat from the flue gas into usable electrical energy without impairing the primary function of the flare, which is the safe combustion of excess gases. A plate heat exchanger is attached around the tip of the flare stack using a supporting frame that is also attached to the derrick structure as shown Fig 2. The plate heat exchanger (PHE) serves as the interface for mounting the TEGs, which are attached to the PHE in array configuration. As the hot side of the TEGs absorbs heat from the flue gases, a temperature gradient is created across the TEGs, allowing them to generate a DC electrical energy output. The DC electrical energy generated by the TEGs is harvested and stored in a container energy storage system (CESS). CESS is a modular unit designed to store electrical energy within a standard shipping container. The container consists of array of batteries integrated with inverter power conversion system (PCS), MPPT control units, and cooling systems all housed within the container. The MPPT control units manage the charge and discharge cycles of the batteries, ensuring stable power output by maximizing the energy extracted from the TEGs through maximum power point tracking. The inverter PCS converts the DC electrical energy generated by the TEG modules into AC electrical.

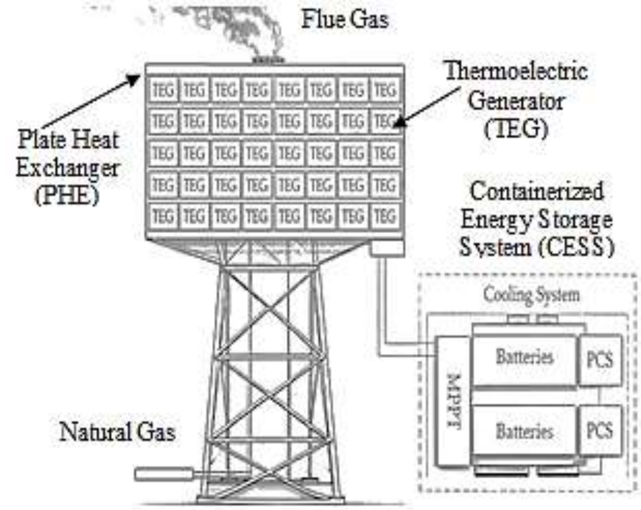

Fig.2: *Flaring System Integrated with TEH System*

2.3 Stoichiometric Analysis of the Flare Gas Combustion

Flaring is a high-temperature oxidation process used to burn combustible components of waste gases from industrial operations. Natural gas constitutes over 95% of the waste gases flared. In complete combustion, gaseous hydrocarbons react with atmospheric oxygen to form carbon dioxide (CO_2) and water. In practice, gas flaring rarely achieves complete combustion (100% combustion efficiency) due to factors like wind speed, gas exit velocity, and poor mixing of air, making it functionally an incomplete combustion process [13]. In Nigeria, natural gas reserves consist of both associated and non-associated gas, largely classified as sweet gas due to low sulfur levels [14]. The incomplete combustion of sweet gas without formation of oxides of nitrogen (NOx) that is mostly experienced in Nigeria oil fields is given by the equation [11]:

$$\left[aCH_4 + bC_2H_6 + cC_3H_8 + dC_4H_{10} + eC_5H_{12} + fN_2 + gCO_2\right] + \alpha\left[O_2 + 3.76N_2\right] \rightarrow \eta xCO_2 + \eta\frac{y}{2}H_2O + (1-\eta)xCO + (1-\eta)\frac{y}{2}H_2 + fN_2 + gCO_2 + 3.76\alpha N_2 \quad (1)$$

where a - g = volumetric fractions of the natural gas constituents (Table1), α = stoichiometric air coefficient, η = combustion efficiency, x = total number of carbon atoms in the fuel mixture, y = total number of hydrogen atoms in the fuel mixture. Combustion efficiency of a flare is the measure of effectiveness with which the combustible gases are burned within the gas flare system. Properly operated flares achieve at least 98% combustion efficiency in the flare plume [15]. N_2 contained in the fuel and combustion air is assumed inert and appears unchanged in the products, while CO_2 in the contained in the fuel also assumed inert and appears unchanged in the products. The combustion reaction provides the thermodynamic basis for evaluating flare heat release, which defines the available thermal energy input to the TEH system.

International Journal of Academic Engineering Research (IJAER)
ISSN: 2643-9085
Vol. 10 Issue 8 August - 2026, Pages: 23-32

2.4 Evaluation of heat harvested by the TEH system

Figure 3 depicts the control-volume used for evaluating flare heat release.

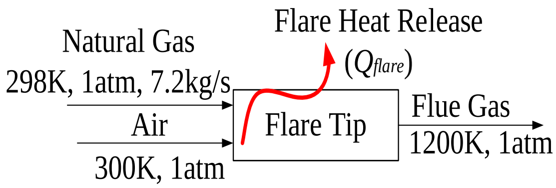

Fig 3: *Control-Volume For Evaluating Flare Heat Release [16][17]*

The heat released during combustion is determined using standard enthalpies of formation, as expressed in (2) [18].

$$\Delta H^o_{comb} = \sum_p n_p \left(h^o_f + h - h^o\right)_p - \sum_r n_r \left(h^o_f + h - h^o\right)_r \quad (2)$$

where n_p = respective stoichiometric coefficients of components in the product, h^o_f = enthalpy of formation, $h - h^o$ = difference in enthalpy for a particular temperature and that of the reference temperature, n_r = respective stoichiometric coefficients of components in the reactant. The flare heat released is given by (3) [18]

$$\dot{Q}_{flare} = \frac{\dot{m}_{ng}}{M_{ng}} \left|\Delta H^o_{comb}\right| \quad (3)$$

where M_{ng} = molecular weight of the natural gas (kg/kmol), $\dot{m}_{ng}$ = mass flow rate of the natural gas (kg/s). The molecular weight of the natural gas is calculated using (4) [18]

$$M_{ng} = \frac{\sum m_i}{\sum N_i}$$

(4)

where m_i = mass of component of the natural gas, N_i = number of moles of component of the natural gas. The heat harvested by the TEH system is defined by (5)

$$\dot{Q}_{TEH} = \xi \times \dot{Q}_{flare}$$

(5)

where ξ = heat exchanger effectiveness, accounting for radiative losses, flue gas dispersion, and geometric constraints at the heat exchange interface.

2.5 Estimation of the Heat Exchanger Effectiveness

Heat transfer from the flue gas to the TEH system occurs predominantly through thermal radiation, supplemented by convective heat transfer from the flue gas stream and conductive heat transfer across the walls of the PHE and TEGs. The radiative heat transfer is expressed by (6)[19]

$$\dot{Q}_{rad} = \varepsilon \times \sigma \times A \times \left(T^4_{flare} - T^4_{PHE}\right) \quad (6)$$

where ε = emissivity of the radiating surface, σ = Stefan-Boltzmann constant, which has a numerical value of 5.67×10−8 W m−2K−4, A = exposed surface area of the PHE, Tflare = flue gas temperature, TPHE = surface temperature of the of the PHE. Emissivity of the radiating surface is a dimensionless quantity between 0 and 1, representing the effectiveness of the surface in emitting thermal radiation. The emissivity of carbon steel used for the construction of the PHE is 0.92 at a temperature of 1200K [20].

The convective heat transfer from the flue gas stream and conductive heat transfer across the walls of the PHE and TEGs are determined using Fig. 4 as follow:

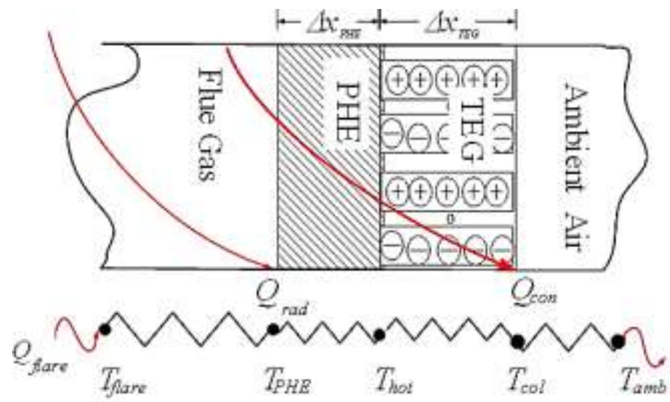

Fig 4: *Schematic of the Heat Transfers to TEG [21]*

The combined convective and conductive heat transfer to the cold side of the TEG can be calculated using (7)[19]

$$\dot{Q}_{conv+cond} = \frac{T_{flare} - T_{col}}{\dfrac{1}{h_{flare}A_{PHE}} + \dfrac{\Delta x_{PHE}}{k_{PHE}A_{PHE}} + \dfrac{\Delta x_{TEG}}{k_{TEG}A_{TEG}}} \quad (7)$$

where T_{col} = cold side temperature of the TEG, h_{flare} = convective heat transfer coefficient of flue gas, A_{PHE} = area of the PHE, Δx_{PHE} = thickness of the PHE, k_{PHE} = thermal conductivity of the PHE, Δx_{TEG} = thickness of the TEG, k_{TEG} = thermal conductivity of the TEG, A_{TEG} = Area covers by of the TEG. The convective heat transfer coefficient of the flue gas flowing through a pipe of diameter 0.677m at a temperature of 1200K and a pressure of 1 atm, with a mass flow rate of 7.2kg/s under turbulent flow conditions, is estimated to be 88W/m²K. Thus, the effectiveness of the PHE was evaluated by relating the combined radiative, convective, and conductive heat transfer rates to the maximum available thermal energy of the flare stream, as defined in (8)[16]

$$\xi = \frac{\dot{Q}_{rad} + \dot{Q}_{conv+cond}}{\dot{Q}_{flare}} \quad (8)$$

International Journal of Academic Engineering Research (IJAER)
ISSN: 2643-9085
Vol. 10 Issue 8 August - 2026, Pages: 23-32

2.6 Thermoelectric Power Generation

The power generated from the TEH system can be calculated using (9)[22]

$$P_{TEH} = \eta_{TEG} \times \dot{Q}_{TEH} \quad (9)$$

where η_{TEG} = energy conversion efficiency of the TEG. The total number of TEGs mounted on the PHEs is determined using (10) [22]

$$N_{TEG} = \frac{P_{TEH}}{P_{TEG}} \quad (10)$$

where P_{TEG} = rated power out of the TEG.

2.7 Thermoelectric Energy Harvested

The thermoelectric energy harvested is the net usable electrical energy output of the TEH system. It is expressed as the product of the the electrical energy generated by the TEGs and the combined efficiencies of the power electronics, which includes MPPT charge controller, inverters as shown in Fig 2. (11) [23].

$$E_{TEH} = P_{TEH} \times \Delta t \times \eta_{MPPT} \times \eta_{PCS} \quad (11)$$

where Δt = duration of the energy harvesting period, η_{MPPT} = efficiency of MPPT charge controller in the CESS, η_{PCS} = conversion efficiency of inverters in the CESS. The capacity of the CESS required for the TEH system is given by (12)[23]

$$C_P = \frac{E_{TEH}}{\eta_{BAT} \times DOD}$$

(12)

where η_{BAT} = charging efficiency of the batteries, DOD = depth of discharge of the batteries.

2.8 Simulation of Heat Distribution to the TEH System

To evaluate the thermal harvesting potential, a simulation was conducted to analyze heat transfer from the flare stack to the integrated TEH system. The system geometry was developed as a CAD model in SOLIDWORKS, and a conjugate heat transfer formulation was implemented to couple radiative, convective, and conductive heat transfer mechanisms between the high-temperature flue gas and the PHE–TEG assembly. Thermal radiation from the flame was treated as the dominant mode at elevated temperatures, while convection is from the buoyant upward flow of combustion gases and entrained ambient air. The numerical results (Fig 5) provide the spatial distributions of temperature across the PHE surface and TEG interface, enabling the assessment of thermal gradients, heat capture effectiveness, and the overall performance of the waste thermal energy harvesting system.

2.9 Economic and Environmental Performance Analysis

To assess the sustainability of the proposed TEH system, two key performance indicators are employed: Payback Period (PBP) for economic feasibility and Carbon Emission Reduction (CER) for environmental impact. The PBP estimates the time required for the energy savings to offset the initial capital investment, while the CER quantifies the total offset of CO_2 equivalent emissions achieved through waste heat recovery. The PBP and CER are calculated using (13) and (14), respectively [22][24].

$$PBP = \frac{C_{sys} \times \left(1 + cf_{om}\right)}{E_s \times C_{1kWh}} \quad (13)$$

and

$$CER = E_s \times Ef \quad (14)$$

where C_{sys} = total cost of the TEH system, cf_{om} = annual operation and maintenance cost factor, E_s = annual energy saved by the TEH system, C_{1kWh} = cost of one-kilowatt hour, which is considered based on its price in Nigeria, Ef = emission factor ($kgCO_2eq/kWh$). The annual operation and maintenance cost factor is expressed as a percentage of the initial investment cost, with standard values ranging from 1% to 4% [25]. Nigeria's average carbon emission factor for grid electricity is 0.573kgCO2eq/kWh [26]

3. RESULTS AND DISCUSSIONS

The results of the study are presented and discussed as following subsections:

3.1 Analysis of the Flare Gas Combustion

The flare gas combustion is analyzed by determining the stoichiometric coefficients in (1), using composition of natural gas in Table 1, and combustion efficiency of 98%. The stoichiometric coefficients are determined thus:

Balancing C:

0.941532 + 0.027801(2) + 0.016582(3) + 0.007791(4) + 0.002971(5) = (0.98)2x + (1-0.98)x

x =1.0929

Balancing H:

0.941532(4) + 0.027801(6) + 0.016582(8) + 0.007791(10) + 0.002971(12) = (0.98)y+ (1-0.98)y

y = 4.1792

Balancing O:

2α = (0.98)2x + (1-0.98)y/2 + (1-0.98)x

α = 1.1034

Thus, (1) is re-written as follows:

$$\begin{bmatrix} 0.9415CH_4 + 0.0278C_2H_6 + 0.0166C_3H_8 + 0.0078C_4H_{10} \\ + 0.0029C_5H_{12} + 0.0011N_2 + 0.0022CO_2 \end{bmatrix} + 1.1034\left[O_2 + 3.76N_2\right] \rightarrow \begin{bmatrix} 1.0710CO_2 + 2.0478H_2O + 0.0218CO + \\ 0.0419H_2 + 0.0011N_2 + 0.0022CO_2 + 7.9639N_2 \end{bmatrix}$$

3.2 Analysis of the Flare Heat Released

Using (2), noting that the natural gas and air enter the flare stack at a pressure of 1atm, and temperatures of 298K and

International Journal of Academic Engineering Research (IJAER)
ISSN: 2643-9085
Vol. 10 Issue 8 August - 2026, Pages: 23-32

300K, respectively; and flame temperature for natural gas flaring is 1200K (from Fig 3). The heat released during combustion is analyzed as shown in Table 2.

Table 2: Authors' Computation Using Standard Values from JANAF Thermochemical Tables

Reactant					**Product**				
Comp	n_e	h_f^o $(kJ/kmol)$	$(h_{300}-h_{298})$ $(kJ/kmol)$	$n_p(h_f^o+h_{300}-h_{298})$ $(kJ/kmol)$	Comp	n_r	h_f^o (kJ/mol)	$h_{1200}-h_{298}$ $(kJ/kmol)$	$n_r(h_f^o+h_{2400}-h_{298})$ $(kJ/kmol)$
CH_4	0.9415	-74850	-	-70471.275	CO_2	1.0710	-393520	79328	-336499.632
C_2H_6	0.0278	-84680	-	-2354.104	H_2O	2.0522	-241820	62876	-367228.877
C_3H_8	0.0166	-103850	-	-1723.91	CO	0.0218	-110530	49470	-1331.108
C_4H_{10}	0.0078	-126150	-	-983.97	H_2	0.0419	0	46219	1936.5761
C_5H_{12}	0.0029	-146440	-	-424.676	N_2	7.9639	0	57651	459126.7989
O_2	2.1181	0	8736	18503.7216					
N_2	7.9639	0	8723	69469.0997					
$\sum_R$				12014.8863	$\sum_P$				-243996.241

From Table 2, heat of combustion of the natural gas is calculated thus:

$$\Delta H^o_{Comb} = -243996.241 - 12014.8863$$

$$= -256011.1273 kJ/kmol$$

The molecular weight of the natural gas of the flare gas is analyzed as shown in Table 3, noting that the numbers of moles are obtained from the percentage composition by volume of the natural gas (from Table 1).

Table 3: Molecular Weight of the Natural Gas

Comp	**Number of Mole (kmol)**	**Molar mass (kg/kmol)**	**Mass (kg)**
CH_4	94.1532	16	1506.451
C_2H_6	2.7801	30	83.403
C_3H_8	1.6582	44	72.9608
C_4H_{10}	0.7791	58	45.1878
C_5H_{12}	0.2971	72	21.3912
N_2	0.1141	28	3.1948
CO_2	0.2182	44	9.6008
$\sum$	**100**		**1742.19**

.

Applying (4), where Σm_i = 1742.19kg, ΣN_i = 100$kmol$ (from Table III), the molecular weight of the natural gas is calculated thus:

$$M_{ng} = \frac{1742.19}{100} = 17.4219 kg/kmol$$

Using (3), flare heat released during combustion is determined as follows: M_{ng} = 17.4219$kg/kmol$, $\dot{m}_{ng}$ = 7.2kg/s (from Fig 3), $\Delta H^o_{Comb} \approx -256011\, kJ/kmol$

$$\dot{Q}_{flare} = \frac{7.2}{17.421} \times 256011 \approx 105808 kW \approx 106 MW$$

3.3 Analysis of the Heat Harvested by the TEH system

The heat harvested by the TEH system is determined from the effectiveness of the PHE as follows:

Applying (6), the radiative heat transfer to the PHE is calculated as follows: ε = 0.92, $\sigma = 5.67\times10^{-8}\ W\,m^{-2}K^{-4}$, A = 3m × 3m (dimensions of the PHE) T_{flare} = 1200K, T_{PHE} = 300K

$$\dot{Q}_{rad} = 0.92 \times 5.67 \times 10^{-8} \times (3\times3) \times (1200^4 - 300^4)$$

$= 969702.678W \approx 970kW$

Applying (7), the convective and conductive heat transfer to the cold side of the TEGs was evaluated using the following parameters: T_{flare} =1200K (from Fig 3), T_{col} =322K [27] h_{flare} = 88W/m^2K. The PHE, fabricated from carbon steel, has thickness Δx_{PHE} = 0.0021m, thermal conductivity k_{PHE} = 35W/mK, and surface area, A_{PHE} = 9m^2. The TEGs have thickness Δx_{TEG} = 0.0079m, thermal conductivity k_{TEG} = 1.75W/mk [27], and effective area A_{TEG} = 8.55m^2, assuming 95% coverage of the available PHE surface area.

$$\dot{Q}_{conv+cond} = \frac{1200-322}{\frac{1}{88\times9} + \frac{0.0021}{35\times9} + \frac{0.0079}{8.55\times1.75}}$$

$$= 488516.1W \approx 489kW$$

Applying (8), the effectiveness of the PHE is determined as follows:

$\dot{Q}_{flare}$ = 105808kW, $\dot{Q}_{conv+cond}$ = 489kW, $\dot{Q}_{rad}$ = 970kW

$$\xi = \frac{489+970}{105808} \approx 0.014$$

Using (5), the heat harvested by the TEH system is determined thus: $\dot{Q}_{flare}$ = 105808kW, ξ = 0.014

$$\dot{Q}_{TEH} = 0.14 \times 105808 \approx 14813.12kW \approx 15MW$$

The results indicate that radiative heat transfer constitutes the primary heat flux to the PHE, which is consistent with the operating conditions of elevated flare stacks. Although the initial radiative heat input of 970kW is reduced to a net convective–conductive heat transfer rate of 489kW due to cumulative thermal resistances across the plate wall of the PHE and TEG layers, the system maintains a thermal effectiveness of 1.4%. Despite this relatively low effectiveness, the high flare thermal energy release of approximately 106MW provides a substantial recoverable waste heat potential of about 15MW.

3.4 Analysis of Thermoelectric Power Generation

Applying (9) and (10), the thermoelectric power output of the TEH system and the corresponding number of TEGs required are evaluated, respectively, as follows: η_{TEG} = 0.07, recent commercial TEGs, fabricated from skutterudite materials, can attain thermoelectric conversion efficiencies up to 7% , and each TEG is rated at $P_{TEG} = 30W$ [27], $\dot{Q}_{TEH} = 15MW$

$$P_{TEH} = 0.07 \times 15 = 1.1MW$$

and $$N_{TEG} = \frac{1100000}{30} \approx 37{,}000$$

Applying (11) and (12), the thermoelectric energy harvested from the TEH system and the capacity of the CESS required for the TEH system are determined, respectively, as follows: $P_{TEH} = 1.1MW$, $\eta_{MPPT} = 0.98$, $\eta_{PCS} = 0.99$, $DOD = 0.9$, $\eta_{BAT} = 0.95$ [28], $\Delta t = 24$, in high oil-producing regions such as the Niger Delta, gas flaring operations frequently run continuously up to 24 hours per day [29].

$$E_{TEH} = 1.1 \times 24 \times 0.98 \times 0.99 \approx 26MWh$$

and $$C_P = \frac{26}{0.9 \times 0.95} \approx 30MWh$$

From the analysis, the integrated TEH system is capable of generating approximately 1.1*MW* of DC electrical power using about 37,000 TEG modules, each with dimensions of 50*mm* × 50*mm* × 7.9*mm*, arranged in a series–parallel configuration on the external surface of the PHE around the flare stack tip. This configuration yields approximately 26*MWh* of usable energy per day, which can be stored in a 30*MWh* CESS comprising three 40-ft containers rated at 10 *MWh* each.

3.5 Thermal Simulation Result

Fig. 5 presents the thermal simulation profile, illustrating the temperature distribution from the flare stack tip through the PHE and across the TEGs.

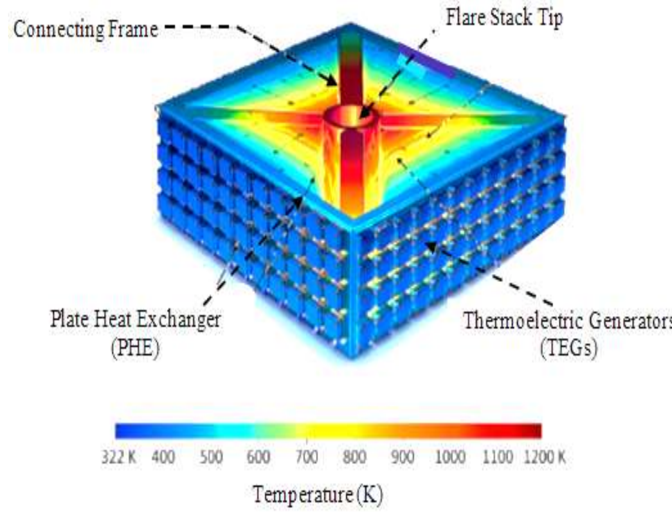

Fig 5: *Temperature Distribution from the flare stack Tip*

The contour plot indicates a thermal gradient originating at the flare stack tip, with a peak temperature of approximately 1200 K. This high-temperature serves as the primary driving force for thermal energy harvesting. As heat propagates through the PHE, the temperature progressively decreases from 1200K to 600K (red-to-green regions), demonstrating effective heat transfer and relatively uniform thermal distribution across the PHE surfaces. Such uniformity is essential for minimizing thermal mismatch losses among TEGs connected in a series–parallel configuration. At the TEG interfaces, the temperature further decreases to the range of 600K to 322K (green-to-blue regions), with 322K defined as the imposed cold-side boundary condition. The sustained temperature differential across the system confirms the capability of the integrated flare–TEH systems to maintain the substantial thermal gradient required for efficient thermoelectric power generation.

3.6 Economic and Environmental Performance Results

The summary of the capital cost associated with integrating the TEH system into the flare system is presented in Table 4.

Table 4: Cost of Integrated Flare-TEH System

Description	Quantity	Rate ($)	Amount ($)
Fabrication of PHE		Lump Sum	450.00
Purchase of 30 W TEGs	37000	85.25	3154250.00
Integration of TEGs and PHE		Lump Sum	150.00
Integration of TEH and Flaring Systems		Lump Sum	300.00
Purchase of 10 MWh CESS	3	200,000	600,000.00
Cable and Accessories		Lump Sum	840.00

Installation of CESS		Lump Sum	280.00
Miscellaneous		Lump Sum	150.00
Total			**3,756,420.00**

Applying (13), the payback period is calculated as follows: C_{sys} = \$3,756,420.00 (Table IV), E_s = 26000kWh/day × 365day/year, = 9,490,000*kWh/year*, cf_{om}= 0.01 C_{1kWh} = \$0.14/*kWh* [30]

$$PBP = \frac{3756420 \times (1 + 0.01)}{9490000 \times 0.14} \approx 3$$

Applying (14), the amount of carbon emission mitigated was, determined as follows; E_s = 9,490,000*kWh/year*, E_f = 0.573$kgCO_2eq/kWh$

$$CER = 9490000 \times 0.573$$

$$= 5{,}437{,}770 kgCO_2eq/year$$

The economic and environmental performance results indicate that the proposed system can be implemented at an estimated capital cost of \$3,756,420, with a simple payback period of approximately 3 years. The system is projected to mitigate about 5,437,770 kg of CO_2 emissions annually. These results demonstrate the financial viability of the project, characterized by relatively short payback duration, while simultaneously delivering substantial environmental benefits through significant carbon emission reduction.

4. CONCLUSIONS

This study explores the development prospects of waste thermal energy harvesting from gas flaring systems using TEGs. The key finding of this study are summarized as follows:

- The radiative heat transfer constitutes the primary heat flux to the PHE, which is consistent with the operating conditions of elevated flare stacks. Although the initial radiative heat input of 970*kW* is reduced to a net convective–conductive heat transfer rate of 489*kW* due to cumulative thermal resistances across the plate wall of the PHE and TEG layers, the system maintains a thermal effectiveness of 1.4%. Despite this relatively low effectiveness, the high flare thermal energy release of approximately 106*MW* provides a substantial recoverable waste heat potential of about 15*MW*.
- The integrated TEH system is capable of generating approximately 1.1*MW* of DC electrical power using about 37,000 TEG modules, each with dimensions of 50*mm* × 50*mm* × 7.9*mm*, arranged in a series–parallel configuration on the external surface of the PHE around the flare stack tip. This configuration yields approximately 26*MWh* of usable energy per day, which can be stored in a 30*MWh* CESS comprising three 40-ft containers rated at 10 MWh each.
- Thermal simulation results demonstrate a progressive temperature decrease from 1200*K* at the flare tip to approximately 600*K* across the PHE–TEG interface, indicating effective heat propagation and relatively uniform temperature distribution. Such uniformity is essential for minimizing thermal mismatch losses among series–parallel connected TEGs and sustaining the temperature gradient required for thermoelectric power generation.
- The proposed system requires an estimated capital investment of \$3,756,420 and achieves a simple payback period of approximately 3 years. Environmentally, the system is projected to mitigate about 5,437,770 kg of CO_2 emissions annually.

In conclusion, these findings confirm that integrating a TEH system with a flare system is technically feasible, economically viable, and environmentally beneficial. Such integration provides a pathway for renewable power generation from flare waste thermal energy while simultaneously mitigating thermal pollution and reducing carbon emissions.

ACKNOWLEDGMENT

The authors gratefully acknowledge the cooperation and support received from the onsite personnel at the Soku gas plant logistics base, Rivers State, Nigeria, during the course of this study.

REFERENCES

[1] L. B. Kong, T. Li, H. H. Hng, F. Boey, T. Zhang, and S. Li. (2014). Waste thermal energy harvesting (I): Thermoelectric effect. Waste Energy Harvesting: Mechanical and Thermal Energies. Springer, Berlin, Heidelberg, pp. 263–403. [Online]. Available: https://doi.org/10.1007/978-3-642-54634-1

[2] C. E. Ogwu, F. M. Oluwaferanmi, and A. I. Johnson. (2021). Impact of gas flaring on climate change (A case study of Niger Delta region of Nigeria). Global Scientific Journal. [Online]. 9(5), pp. 1781–1789. Available: http://www.globalscientificjournal.com

[3] N. V. Toan, N. D. K. Tran, T. T. K. Tuoi, S. M. Said, M. F. M. Sabri, and T. Ono. (2025, Aug. 15). Nanoengineering silicon materials by metal-assisted chemical etching for thermal energy harvesting. Materials Science in Semiconductor Processing. [Online]. 195, Art. no. 109622, pp. 1–14. Available: https://doi.org/10.1016/j.mssp.2025.109622.

[4] Y. Lan, J. Lu, and S. Wang. (2024, Apr. 1). An experimental study on the performance of TEGs using uniform flow distribution heat exchanger for low-grade thermal energy recovery. Energy. [Online]. 292, Art. no.

130506. Available: https://doi.org/10.1016/j.energy.2024.130506

[5] J. S. Jadhao and D. G. Thombare. (2013). Review on exhaust gas heat recovery for I.C. engine. International Journal of Engineering Innovation and Technology. [Online]. 2(12), pp. 93–100. Available: https://www.ijeit.com/vol%202/Issue%2012/IJEIT1412201306_18

[6] I. Petsagkourakis, K. Tybrandt, X. Crispin, I. Ohkubo, and N. Satoh. (2018). Thermoelectric materials and applications for energy harvesting power generation. Science and Technology of Advanced Materials. [Online]. 19(1), pp. 836–862. Available: https://doi.org/10.1080/14686996.2018.1530938.

[7] A. Faraj, H. Jaber, K. Chahine, J. Faraj, M. Ramadan, H. El Hage, and M. Khaled, "New concept of power generation using TEGs: Thermal modeling, parametric analysis, and case study," Entropy, vol. 22, no. 5, p. 503, Apr. 2020, pp. 1–16, doi: 10.3390/e22050503.

[8] H. Jouhara, N. Khordehgah, S. Almahmoud, B. Delpech, and A. Chauhan, "Waste heat recovery technologies and applications," Thermal Science and Engineering Progress, vol. 6, no. 4, pp. 268–289, 2020, doi: 10.1016/j.tsep.2018.04.017.

[9] Department of Petroleum Resources. (2018, Jul.). 2016 oil & gas annual report: Nigerian industry Annual Statistical bulletin. [Online]. Available: https://www.nuprc.gov.ng/wp-content/uploads/

[10] V. N. Otugo and A. R. C. Amakiri. (2024, May–Jun.). Patterns and variability of rainfall and temperature in Port Harcourt Metropolis, Rivers State, Nigeria. SSRG International Journal of Recent Engineering Science. [Online]. 11(3), pp. 138–142. Available: https://doi.org/10.14445/23497157.

[11] O. S. Ismail and G. E. Umukoro. (2014). Modelling combustion reactions for gas flaring and its resulting emissions. Journal of King Saud University – Engineering Sciences. [Online]. 6(2), pp. 130–140. Available: http://dx.doi.org/10.1016/j.jksues.2014.02.003.

[12] X. Sheng, H. Zhang, Y. Bao, and C. Ling. (2016, Jan.). Finite element checking of flange connection in integral hoisting of flare stack. Presented at the 2016 International Conference on Advanced Electronic Science and Technology (AEST 2016). [Online]. Available: https://doi.org/10.2991/aest-16.2016.50.

[13] D. M. Leahey, K. Preston, and M. Strosher. (2002, Jan.). Theoretical and observational assessments of flare efficiencies. Journal of the Air & Waste Management Association. [Online]. 51(12), pp. 1610–1616. Available: https://doi.org/10.1080/10473289.2001.10464390

[14] Nigerian Upstream Petroleum Regulatory Commission. (2024, Apr.). 2023 annual report. [Online]. Available: https://www.nuprc.gov.ng/wp-content

[15] B. Peebles and P. Stockton. (2022, Oct.). Offshore flares: measurement and calculation of combustion efficiency, methane and CO_2e emissions. Presented at the Global Flow Measurement Workshop 2022, Aberdeen, Scotland. [Online]. Available: https://www.researchgate.net/publication/368839792

[16] X. Qian, S. W. Lee, and Y. Yang. (2021). Heat transfer coefficient estimation and performance evaluation of shell and tube heat exchanger using flue gas. Processes. [Online]. 9(6), pp. 1–19. Available: https://doi.org/10.3390/pr9060939.

[17] Y. A. Çengel and M. A. Boles. (2019). Thermodynamics: An Engineering Approach, 9th ed. New York, NY, USA: McGraw-Hill.

[18] M. J. Moran, H. N. Shapiro, D. D. Boettner, and M. B. Bailey. (2010). Fundamentals of engineering thermodynamics, 7th ed. Hoboken, NJ: John Wiley & Sons, Inc.

[19] T. L. Bergman, A. S. Lavine, F. P. Incropera, and D. P. DeWitt. (2011). Fundamentals of Heat and Mass Transfer, 7th ed. New Jersey: John Wiley & Sons.

[20] Omega Engineering. (2000). Emissivity of common materials. [Online]. Available: https://www.omega.co.uk/literature/transactions/volume

[21] B. Gbaarabe, J. I. Sodiki, B. T. Lebele-Alawa, and B. Nkoi. (2025, Aug.). Performance optimization of a thermoelectric energy harvesting system utilizing waste heat from an internal combustion engine. Applied Engineering and Technology. [Online]. 4(2), pp. 1–13. Available: https://doi.org/10.3176/aet.v4i2.2093.

[22] A. Faraj, H. Jaber, K. Chahine, J. Faraj, M. Ramadan, H. El Hage, and M. Khaled. (2020, May). New concept of power generation using TEGs: Thermal modeling, parametric analysis, and case study. Entropy. [Online]. 22(5), pp. 1–16. Available: https://doi.org/10.3390/e22050503.

[23] B. Gbaarabe and B. Nkoi. (2023). Development and techno-economic analysis of a large-scale speed bump power generation system. International Journal of Sustainable and Green Energy. [Online]. 12(2), pp. 13–20. Available: https://doi.org/10.11648/j.ijrse.20231202.11

[24] B. J. Lee, J. I. Lee, S. Y. Yun, B. G. Hwang, C.S. Lim, and Y.K. Park. (2020). Methodology to calculate the CO_2 emission reduction at the coal-fired power plant: CO_2 capture and utilization applying technology of mineral carbonation. Sustainability. [Online]. 12(18), pp. 1-13. Available: https://doi.org/10.3390/su12187402.

[25] International Renewable Energy Agency, Renewable energy technologies: Cost analysis series, IRENA Working Paper, vol. 1, no. 3, pp. 1–44, 2012. [Online]. Available: https://www.irena.org

[26] Institute for Global Environmental Strategies, List of grid emission factors, ver. 11.0, 2022. [Online].

Available: https://pub.iges.or.jp/pub/iges-list-grid-emission-factors

[27] Furukawa Co., Ltd., Skutterudite thermoelectric materials and modules, Research and Development Division, Materials Research Laboratory, Tsukuba, Japan, 2024. [Online]. Available: https://www.furukawakk.co.jp. Accessed: Feb. 26, 2026.

[28] Greensun Solar Energy Tech Co, "Product details of 20 feet container energy storage system," 2025. [Online]. Available: https://www.greensunbattery.com/bess-20-feet-1mwh-12mwh-container-system. Accessed: Feb. 26, 2026.

[29] J. Conant and P. Fadem, "Gas flare," in A Community Guide to Environmental Health, 1st ed., ch. 22. Hesperian Health Guides, 2012. [Online]. Available: https://store.hesperian.org.

[30] Nigerian Electricity Regulatory Commission, "Electricity tariff now N225/kWh," 2024. [Online]. Available: https://nerc.gov.ng. Accessed: Jun. 16, 2024.